5. ROCK RESISTIVITY, CONDUCTIVITY & AND NATURAL ELECTRIC POTENTIAL

RESISTIVITY AND CONDUCTIVITY

5.1. Rock Resistivity in general

5.2. Resistivity of a multy component system

- 5.2.1. Components in rock
- 5.2.2. The relation between F_R and rock porosity
- 5.2.3. Relation between F_R and matrix cementation/compaction
  - 5.2.3.1. Humble and Archie
  - 5.2.3.2. Cementation factor and sediment type
- 5.2.4. The relation between F_R and the water content (S_w)
- 5.2.5. Water saturation calculations using Archie

5.3. Resistivity logging tools

- 5.3.1. Introduction and historical development
- 5.3.2. Electrical Surveys (es)
  - 5.3.2.1. Short normal, Long normal, and Lateral tool
  - 5.3.2.2. SN, LN and Lateral log behaviour
- 5.3.3. Laterolog tools (LL3, LL7 & DUAL LATEROLOG)
- 5.3.3.1. LL3
  - 5.3.3.2. laterolog 7 (LL7)
  - 5.3.3.3. Dual Laterolog
- 5.3.4. Induction Logging
- 5.3.5. Micro-resistivity devices
  - 5.3.5.1. The Microlog (ML)
  - 5.3.5.2. Micro Spherically Focused Log (MSFL)
- 5.3.6. Vertical and horizontal resolution: summary

NATURAL ELECTRIC POTENTIALS

5.1 ROCK RESISTIVITY IN GENERAL

Rock material and rock mass can be classified, for matrix and porosity through its heterogeneity in resistivity. In general a sedimentary rocks shows resistivity by the presence of high conductive and low conductive components. The salinity of water in the pores and the presence or absence of clays and/or shales are important factors in controlling the flow of electric current. Figure 5.1.shows the general relation for a resistance "r" of a material with its ability to impede the flow of electrical current. The resistance is defined as the ratio of the electric field strength and the electric current, or:

$$r = \frac{E}{I} \qquad \text{(eq. 5.1)}$$

With r in Ohm; E in Volt; and I in Ampere. The specific resistance *"R"* is defined as the resistance over a specific volume of matter. Hence, the resistance "r" is multiplied with a surface A and divided by the length L of the specific matter. Specific resistance or resistivity of a substance is defined as *R* or R_O:

$$R = R_o = \frac{E \cdot A}{I \cdot L} \qquad \text{(eq. 5.2)}$$

R is in ohm.m. The conductivity (*C)* is defined as the reciprocal of resistivity, or:

$$C = \frac{1}{R} \qquad \text{with the unity of (ohm.m)}^{-1} \qquad \text{(eq. 5.3)}$$

The unit of conductivity (ohm.m)$^{-1}$ is often replaced by the redefined unit mho/m, or in the metric system S/m (Siemens/m). To avoid very small values, 1 ohm^{-1} is valued as 1000 m.mho (millimho's).

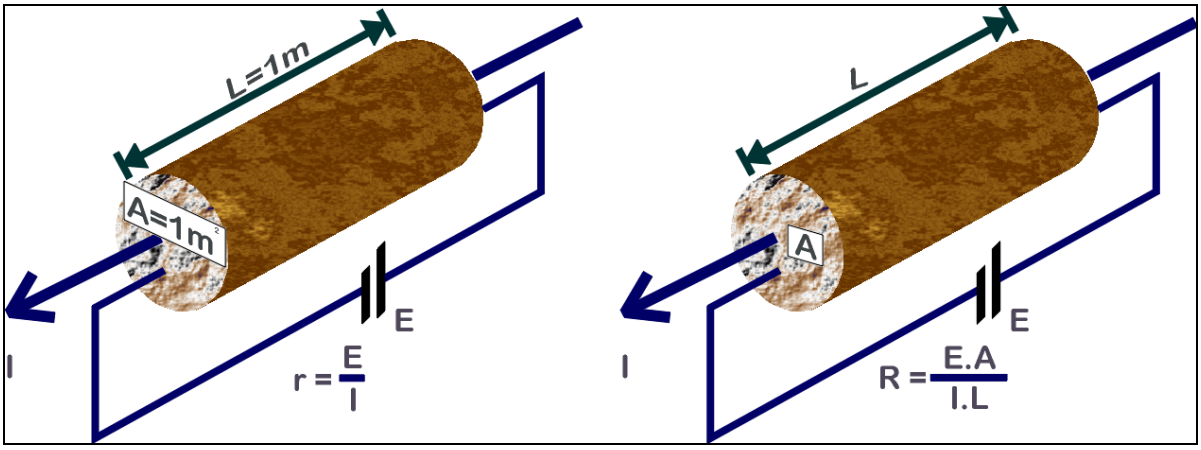

Figure 5. 1: definition of resistance (left) and resistivity (right) of a conducting material.

5.2 RESISTIVITY OF A MULTY COMPONENT SYSTEM

5.2.1 COMPONENTS IN ROCK

Normally a rock, or formation, consist of:

- **Non-conductive components:** like many matrix minerals, such as water-poor silica minerals (quartz, feldspar), carbonates, carbonaceous matter, hydro-carbons and fresh water, and,
- **Conductive components:** such as water bearing silica (shales, clays), ore minerals (magnetite, pyrite, galena as a semiconductor) and brine.

In general the total rock conductivity is controlled by the properties of fluid phase or the pore content or by a multi-component system in which the saturation of the pore space plays an important role. To

characterise the relationship between the components of a rock, or: between the matrix content and the pore content, the generic term **formation resistivity factor** (F or F_R) is brought into being.

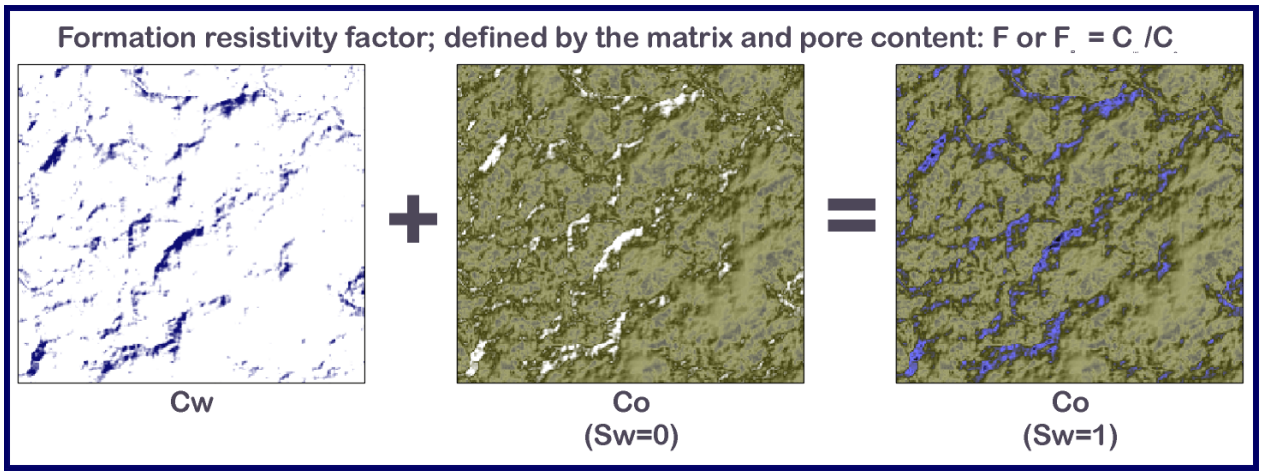

Figure 5. 2: Matrix resistivity and pore resistivity defining the formation factor and total resistivity

5.2.2 THE RELATION BETWEEN F_R AND ROCK POROSITY

When a porous rock sample with porosity φ, as shown in figure 5.2, can be exemplified by an equivalent system of n saturated straight capillary tubes and the relationship between the total cross-sectional area (A) of a block with a length L, and the cross-sectional area of n capillary tubes ($A_n = n.\pi.r_c^2$) of length L, then:

$$A_n = \varphi A \qquad \text{(eq. 5.4)}$$

The resistivity of the brine in the capillary pore space is:

$$R_{w.cap} = \frac{E \cdot A_n}{I_{w.cap} \cdot L} \qquad \text{(eq. 5.5)}$$

Now, as shown in figure 5.2 the formation resistivity factor F is the ratio of the resistivities of the matrix and fluid, or the ratio of the equations 5.2 and 5.5:

$$F = F_R = \frac{R_o}{R_{w.cap}} = \frac{A}{A_n} \cdot \frac{I_{w.cap}}{I_o} \qquad \text{(eq. 5.6)}$$

Here $I_{w.cap} = I_o$ since we assumed the n capillaries equal to the porous rock sample. Combining the equations 5.4 and 5.6 gives the basic dependency between the formation resistivity factor and porosity, or:

$$F = F_R = \frac{1}{\varphi} \qquad \text{(eq. 5.7)}$$

If the tubes are replaced by a more natural kind of pore space, the space between a matrix consisting of sand grains, then the formation resistivity factor will change considerably. A porous system consisting of grains simply has no straight capillary tubes. Thus, the tortuosity factor (τ), as defined in chapter 4: $\tau = \left(\frac{L_a}{L}\right)^2$, where; L is the sample length and L_a is the actual length of the flow path, is combined with equation 5.5:

$$R_{w.cap} = \frac{E \cdot \varphi \cdot A_n}{I_{w.cap} \cdot L} \qquad \text{(eq. 5.8)}$$

If the equations 5.2 and 5.8, for respectively R_O and R_W, are divided by equation 5.4, and the assumption of $I_{w.cap} = I_o$ is applied, then the resulting resistivity factor for gives a relation for tortuosity:

$$F_r = \frac{1}{\varphi} \cdot \frac{L_a}{L} = \frac{\sqrt{\tau}}{\varphi} \qquad \text{(eq. 5.9)}$$

Horizontal or inclined tubes can be compared with a fractured or grain like porous medium, assuming that the total current I_o is the same as the current through the capillaries $I_{w.cap}$. This is possible when a very high resistivity rock is filled with very low resistive water. In that case a capillary tube has to be compared with the current path between the grains. In that specific case the tortuosity (τ) shows the essential difference of the textures and the related formation resistivity factors. (Equations 5.7 and 5.9)

5.2.3 RELATION BETWEEN F_R AND MATRIX CEMENTATION/COMPACTION

In the previous sections the matrix minerals were considered to consist of tubes and grain particles. The related pore space is easy to define. However, in nature the grains often are compacted or cemented by various cementing materials, like; silica, carbonates and clay minerals. These cemented grain fabrics usually have lower porosities and, according to equation 5.9, higher resistivity factors, because of the reduction in porosity.

5.2.3.1 HUMBLE AND ARCHIE

From laboratory tests on the formation resistivity factor (F_R) and porosity (ϕ), a relation was found between these two variables. Using the general form of the expression as used in equation 5.7, they show:

$$F = F_R = \frac{1}{\varphi^m} = \frac{R_o}{R_w} = \frac{C_w}{C_o} \qquad \text{; also named the first Archie equation} \qquad \text{(eq. 5.10)}$$

Here *m* is the cementation factor, which is related to the shape and distribution of pores. For this reason *m* is also called the lithology exponent. For this relation we can make the following comments, assuming a fixed pore fluid resistivity:

- The total rock resistivity R_O decreases with increasing porosity for the same kind of pore-geometry.
- In this case the pore geometry itself can be considered as a function of the lithology and the texture. Moreover, it characterises how the pores are connected. Hence, pores that are very tortuous or poorly connected do have a higher resistivity than a regular well-connected pore geometry.

A cementation factor can be determined by measuring the formation resistivity factor of several samples and plotting the porosities and the formation resistivity factors on double logarithmic paper. A straight-line relationship (figure 5.3) is often found when equation 5.10 is converted to:

$$\log F = -m \log \varphi \qquad \text{(eq. 5.11)}$$

Now *m* is the slope. In compacted sandstones and (homogeneous) chalky rocks *m* has a value of ~2, whereas for highly cemented or compacted silicate-rocks and compact limestones the m increases to values over 3 (table 5.1, 5.2). “m” frequently varies from well to well, due to:

- the lateral heterogeneous character of sediments, even in a formation, and
- variation in burial history in a geological regions.

When *m* is difficult to determine, a constant “*a*” is introduced (figure 5.3). “*a*” depends on all kind of varieties, such as rock type, variation in pore type, quality of the measurement, etc. This adjusted equation, referred to as the Humble formula, also can be used to estimate the formation factor:

$$F = F_R = \frac{a}{\varphi^m} \qquad \text{(eq. 5.12)}$$

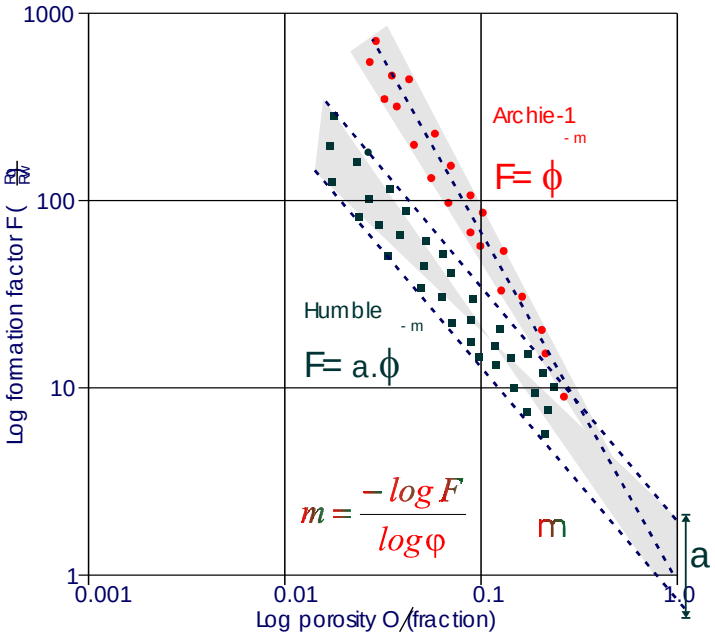

Figure 5. 3: Graphical presentation of the first Archie equation and the revision by Humble.

Again, the best values for both, "a" and "m" are determined by laboratory evaluations. For the siliclastic sediments and the carbonates, the m-values in-situ are higher than under "atmospheric" laboratory conditions.

$$m = \frac{-\log F}{\log \varphi} \qquad \text{(eq. 5.13)}$$

Equation 5.13 shows the effects of compaction on the matrix: less porosity gives less water, and therefore a higher R_O, at a constant R_W.

Consolidation	**atmospheric**	**in-situ**
I BCD, interconnected	2.2	2.4
I BCD, moderate to abundant, poorly interconnected	2.6	2.8
I/II-II, no vugular porosity I/ III-III,	2.0	2.2
I/II-II BC, interconnected I/III-III BCD, moderate, poorer interconnection	2.2	2.4
LIII-II BCD abundant, poorer interconnection I/III-III	2.6	2.8

Table 5. 1: Carbonates Relation of cementation factor (m) and Archie classification.

5.2.3.2 CEMENTATION FACTOR AND SEDIMENT TYPE

After many years of measurements on cores, a wide range of regular values have been found for the cementation exponents of various types of sandstones and carbonates. The tables 5.1 and 5.2 show the atmospheric values and in-situ values for sandstones and carbonates, generally used in log evaluations. The most reliable to validate the above mentioned "m" values is the laboratory analysis of core samples. However this can only be done when cores are available.

- **laboratory measurements performed on plugs cut from cores.**
  For each plug the porosity ϕ and the conductivity C_O of a sample 100% saturated with water of conductivity C_W, is measured. The '*m*' values calculated with equation 5.12 differ slightly from sample to sample even for a very clean homogeneous sand.Therefore they are averaged for the final evaluation.
- **water-bearing reservoirs.**
  When a hydrocarbon column in a reservoir overlies a water leg it is possible to determine the "m" factor from wireline logs alone. The density log, that will be discussed in a coming chapter, provides porosity values, while the rock conductivities C_O. are derived from resistivity logs. The formation water conductivity C_W can be obtained via the spontaneous potential (SP) log (Next topic). The "m" factor can then be calculated using the first Archie equation.

5.2.4 THE RELATION BETWEEN F_R AND THE WATER CONTENT (S_W)

In a hydrocarbon polluted soil, rock formation or an oil and/or gas-bearing zone, pores are filled with highly conductive brine and the hydrocarbons as non-conductive constituents. As shown before, the

Consolidation	Atmospheric	in-situ
very unconsolidated sand shallow potable water reservoirs	1.2	1.2
unconsolidated sand	1.4	1.6
unconsolidated to friable sand	1.5	1.7
friable sandstone	1.6	1.8
hard to friable sandstone	1.7	1.9
hard sandstone	1.8	2.0
very hard sandstone	2.0	2.2

Table 5. 2: Sands and sandstone relation of cementation factor (m) and sand consolidation

rock conductivity (C_O) or rock resistivity (R_O) is a function of water saturation S_W. When a part of the water is replaced by hydro-carbons, the true resistivity, R_t, of the porous rock is larger than the resistivity of a rock that is 100 % saturated with brine (R_O), or, equation 5.10 rewritten as:

$$\varphi^m \cdot C_w = C_o$$

Water saturation related to the porosity and resistivity index
The total resistivity is much higher and there is less available volume for the flow of electric current. Archie proved experimentally that the resistivity factor F_R of a formation partially saturated with brine could be expressed as:

$$S_w = \left(\frac{R_o}{R_w} \right)^{\frac{1}{n}} = \left(\frac{F_r \cdot R_w}{R_t} \right)^{\frac{1}{n}} \qquad \text{(eq. 5.14)}$$

The ratio which defines the amount of hydro-carbon in the pores, next to water, was named the resistivity index I_R , so:

$$I_R = \frac{R_t}{R_o} = \frac{C_o}{C_t} \qquad \text{(eq. 5.15)}$$

If a porous sample is fully saturated with brine, or S_W=1, then the resistivity index is equal to one. If I_R is greater than one then hydrocarbons are filling a part of the pores. Here the resistivity index is a function of the salinity and the amount of brine. To generalise equation 5.14, for less homogeneous textures, it is combined with Humbles relation (eq. 5.12) to:

$$S_w = \left(\frac{a \cdot R_w}{\varphi^m \cdot R_t} \right)^{\frac{1}{n}} \qquad \text{(eq. 5.16)}$$

With; R_t as the true resistivity of formation containing hydrocarbons and formation water; R_o as the resistivity of formation when 100% saturated with water; n as the saturation exponent and I_R as the resistivity index.

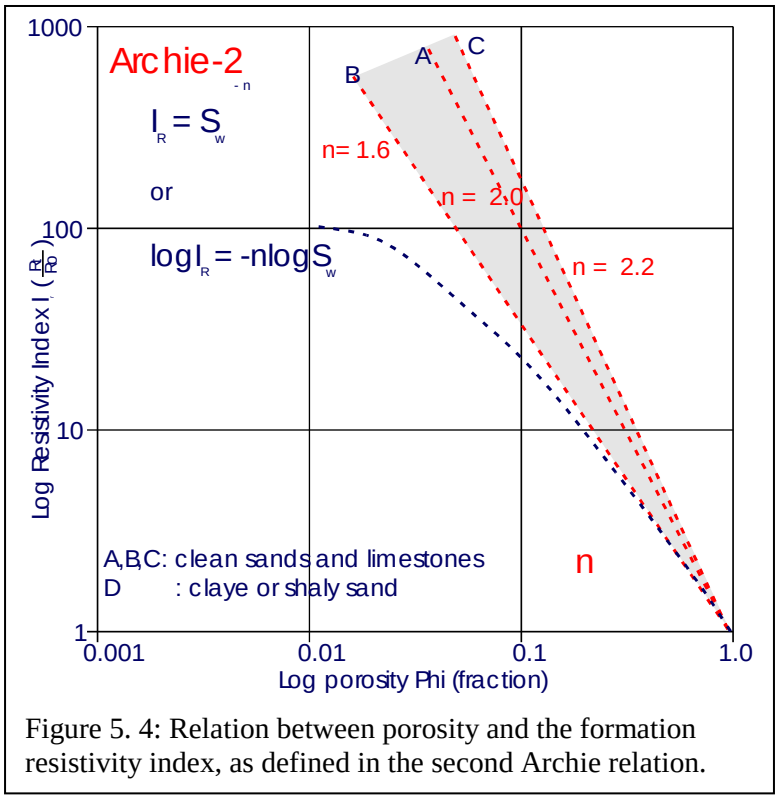

Figure 5. 4: Relation between porosity and the formation resistivity index, as defined in the second Archie relation.

As said before, the relationship between the resistivity index and the water saturation is established by Archie. A properly cleaned and evacuated, sample is saturated with a brine with resistivity R_W and R_O the total resistivity (S_W=1) is measured. The water saturation is decreased stepwise by flushing with oil. After equilibrium is reached at each step, the conductivity R_t is measured again. At each step S_W is calculated from the volume of the expelled water and the porosity. For clean homogenous samples the data points in a double logarithmic plot, usually show a linear trend. The relationship between the ratio of R_O and R_t, the resistivity index I, can be rewritten using the equations 5.14 and 5.15:

$$I_R = \frac{R_t}{R_o} = S_w^{-n} \qquad \text{(eq. 5.17)}$$

Here "n" is the slope of the linear trend in a double logarithmic plot, called the saturation exponent. The majority of the n-values range from 1.6 to 2.4. When core measurements are not available, normally the value n = 2 is accepted to be used. The value of n is influenced by:

- wettability,
- overburden pressure,
- fluid type; brine, oil, fresh water
- heterogeneity of fluid distribution, like tortuosity, and,
- the types and amounts of conductive clays (as already shown in figure 5.4).

The following effects of wettability on the saturation exponent are explained:

1. In homogeneous oil-wet systems with low brine saturations large values for "n", of 10 or higher, are possible.

2. If the saturation of the brine is high enough to create a regular thin layer on a grain surface of a porous medium (to build a uninterrupted path for a current flow), then the saturation exponent *n* is basically not subordinate to wettability. This occurs in clean and uniformly water-wet systems. Here the value of *n* is circa 2. In essence *n* remains constant as S_W is lowered to the irreducible value, S_{wi}.

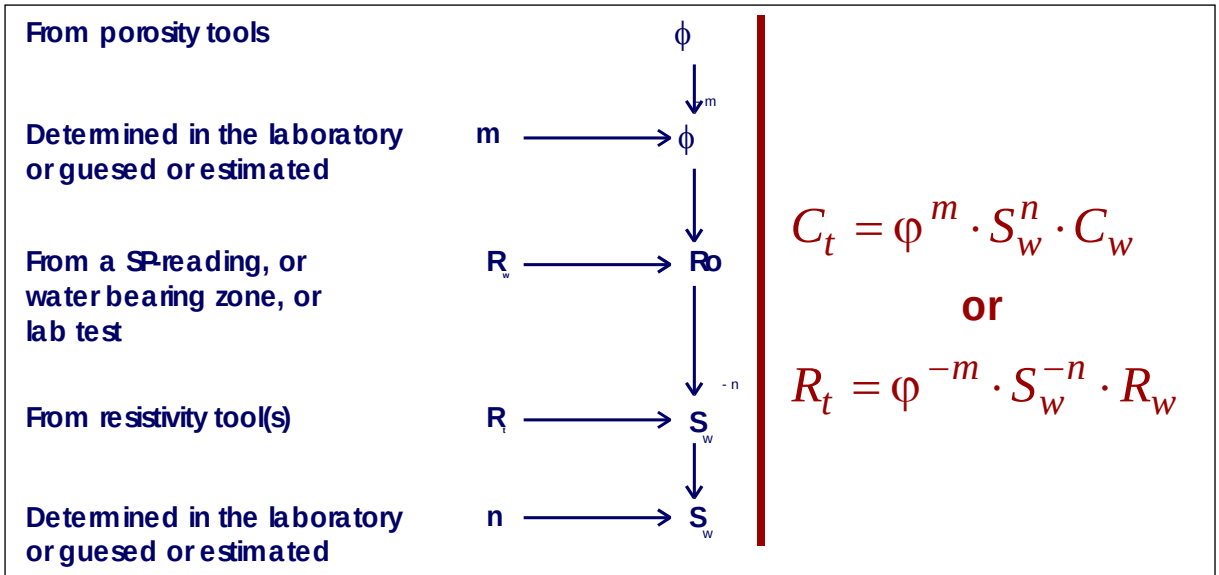

Figure 5. 5: Determination of S_W using the combined Archie equation.

5.2.5 WATER SATURATION CALCULATIONS USING ARCHIE; LABORATORY AND WILD LIFE

When the equations 5.10 and 5.16 are combined and manipulated, the result will be a general equation in which all resistivity and volumetric parameters are used:

$$C_t = \varphi^m \cdot S_w^n \cdot C_w \quad \text{or} \quad R_t = \varphi^{-m} \cdot S_w^{-n} \cdot R_w \qquad \text{(eq. 5.18)}$$

The five parameters required for S_W are (figure 5.5):

1. the porosity ϕ and conductivity C_t , which are measured with wireline logs.
2. the formation water conductivity C_W , which is determined in a water-bearing zone through sampling or with the spontaneous potential (SP) log.
3. the cementation factor "*m*" and saturation exponent "*n*" preferably from laboratory core analysis.

In general in the calculations leading to the water saturation S_W, each input parameter adds to the overall uncertainty. When either the "n" or "m" exponents are estimated too high, or the porosity ϕ to low, the S_W will be, in all cases, too high.

Till now various resistivity parameters are discussed and used to define the relations between physical and textural aspects of porous rock and its content. The measurements in a well normally are performed in a zone around the drill hole. Normally this area is affected by drilling fluid and therefore named the invaded zone or flushed zone. All direct information on porosity and resistivity, that is gathered in this zone, is detected with fluid mixtures from the drill hole. In the adjacent transition zone the pore fluid consists of a blend from the borehole fluid and the virgin zone. The codes as shown in figure 5.6 are normally put to use when petrophysical data are evaluated:

di : diameter of the flushed zone, i.e. the zone through which several pore volumes of filtrate circulated, containing a residual hydrocarbon saturation.
Dj : diameter to the virgin or uninvaded zone.
dh : diameter of the borehole
hmc: thickness of the mud cake
h : thickness of the layer
R_w : resistivity of the formation water in the uninvaded pores
R_{mf} : resistivity of the mud filtrate
R_{mc} : resistivity of the mud cake
R_m : resistivity of the mud

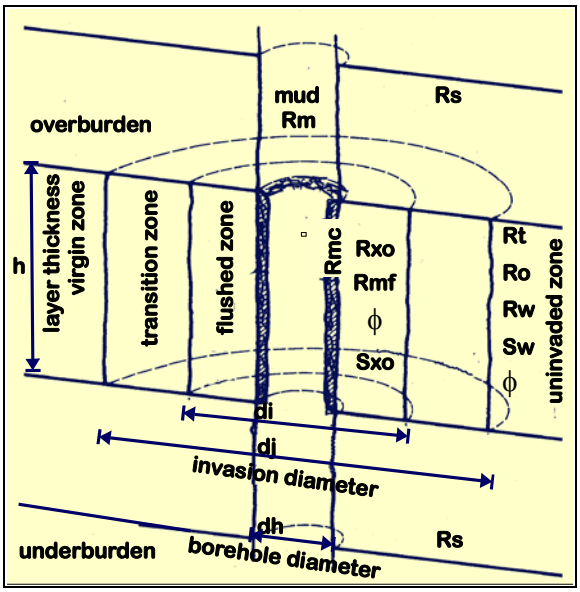

Figure 5. 6: Diagram of the nomenclature in and around a borehole.

Drilling disturbs the equilibrium in the distribution of water and hydrocarbon saturations that is determined by the interaction of gravity and capillary forces in the undisturbed reservoir. As mud filtrate invades permeable formations the conductivity in the invaded zone changes, as discussed in the previous chapters. The shape of this zone is often considered to be cylindrical around the borehole and also assumed to contain water with a conductivity equal to that of the mudfiltrate. The values can be measured on the surface on mud filtrate samples. In relatively impermeable rock, like shales, invasion does not occur. **The flushed zone** is defined as the zone around the borehole where the pores are 100 % filled with mudfiltrate. **The transition zone** contains a mixture of mudfiltrate and original formation fluids. **The virgin zone** only contains original formation water/hydrocarbon saturation. The lateral extent of the flushed zone and the invaded zone are usually not known. Additional conductivity measurements, with different depth of investigation, will therefore be required to locate these zones and compensate for the effect on resistivity measurements, as discussed in the next section.

5.3 RESISTIVITY LOGGING TOOLS

5.3.1 INTRODUCTION AND HISTORICAL DEVELOPMENT

There is a bewildering variation in the design and principles used for resistivity logging. While we usually only want to know one parameter the true resistivity Rt , eleven different resistivity tools will be mentioned in this section. The reason for this avalanche of designs is that the resistivity of the borehole, the mudfiltrate, and adjacent beds all have an effect on the resistivity measured by a tool in the borehole. No single design can fully compensate for all these effects, and a combination of measurements with different tools is required to calculate the illusive R_t .

ELECTRIC SONDE: The first resistivity log, an electrical survey (ES) was run in 1927 by Marcel and Conrad Schlumberger. The ES tool contains 3 lead electrodes held together with ropes. One electrode is used to inject current via the borehole in the formation, and the other two are use to measure the potentials generated by this current. Formation resistivity values can only be obtained under favourable conditions, i.e. slim boreholes, relatively high mud resistivity, shallow invasion and thick beds. This simple tool was already successful in detecting layer boundaries and high resistivities indicative for the presence of oil. The first overseas ES log was already run in Brunei (Borneo) in 1929. ES logs although superseded in Western oil and gas logging operations will still be discussed, because similar tools are used for ground-water operations, and a large proportion of well data in older fields consists solely of ES logs

INDUCTION LOGS: Before the second world war many wells were drilled with muds that consisted of locally available clay and water mixtures with a low salinity. These muds were often incompatible with the shales encountered downhole, which led to clay swelling, large wash-outs, and even caving of wells. In the early fifties oil-base muds were developed that had diesel as the continuous phase and therefore significantly reduced clay problems. However these muds did not conduct electric currents and ES tools with electrodes could not be applied anymore. Induction tools were developed for these circumstances, which derived conductivity values of the formation based on the electromagnetic coupling of transmitter and receiving coils in the logging tool via the conductive rock surrounding non-conductive borehole.

LATEROLOGS: In the same period laterolog tools were developed for high salinity drilling muds, applied to drill through salt layers, in which ES tools are virtually short circuited. The laterologs use arrays of electrodes to focus the current emitted by the centre electrode into the formation, and thereby significantly reduce the effect of the mud. Both the induction and laterolog tools are superior to the older ES tools to obtain a reliable value of the true resistivity of the uninvaded formation.

MICRO RESISTIVITY TOOLS: The micro resistivity tools were introduced to provide an accurate assessment of the resistivity of the invaded zone R_{xo}. These tools have in common that the electrodes are very close together and are mounted on a pad that is pushed against the borehole wall to minimise the effect of the borehole fluid.

5.3.2 ELECTRICAL SURVEYS (ES)

5.3.2.1 SHORT NORMAL (SN), LONG NORMAL (LN), AND LATERAL TOOL DESCRIPTION

Wireline logging tools can evidently not measure subsurface parameters without a borehole to accommodate the tools. The presence of the borehole however severely hampers the determination of the formation resistivity due to the conductivity or lack of conductivity (oil base mud) of the borehole itself. If we could place electrodes in the ground without drilling (a typical thought experiment) we could pass an electric current between electrode "A" embedded in an infinite, homogenous isotropic medium and electrode "B" at an infinite distance. The current would then flow radially outward in all directions as shown in figure 5.7. In this case the equi-potential surfaces are spheres with their centres at the current electrode "A". If we would place another electrode "M" near "A", electrode "M" would then lie on the sphere whose radius is the distance AM. If "M" would be connected through a potentiometer to a remote electrode "N", this meter would then indicate the potential at the sphere of radius AM. For a sphere the potential difference between electrode M and electrode N is as follows :

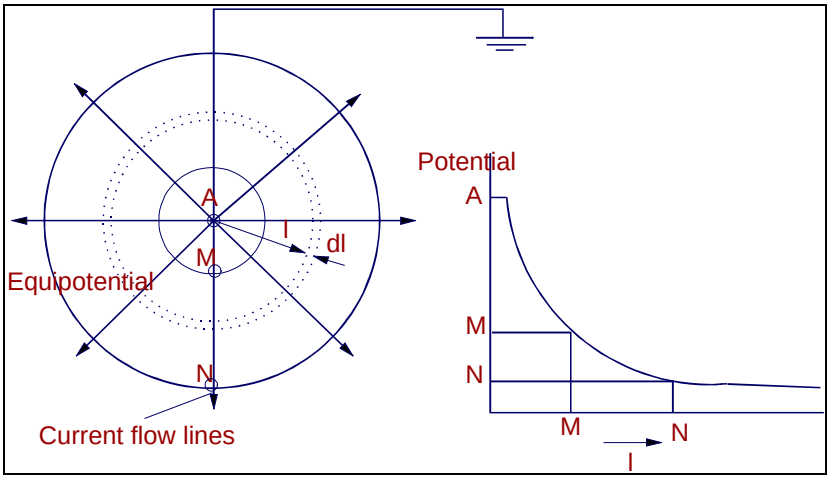

Figure 5. 7: Potential distribution in the radial flow of electricity. (Lynch, 1962)

$$E_m - E_n = \sum_{AM}^{AN} \frac{I.R}{4.\pi.L^2}.dL = \frac{I.R}{4.\pi.AM} \qquad \text{(eq. 5.19)}$$

This can be rearranged as :

$$R = \frac{K_n . \Delta E}{I} \qquad \text{(eq. 5.20)}$$

where K_n is a proportionality factor depending on the electrode spacings. If the tool emits a constant current I and the potential difference ΔE is measured, R can then be calculated. The potentials E_m and E_n are measured by electrodes in the borehole. If the borehole resistivity does not deviate too much from the formation resistivity these potentials correspond to similar potentials in the rock formation, as shown in Figure 5.8 at the left. The greater the distance of the two measuring electrodes from the current electrode A, the deeper these equi-potential spheres reach into the formation. In electric logging the long spacing tools are therefore referred to as the deep penetration tools. The price to pay for the deep penetration is the low vertical resolution. The formulation of equation 5.20 demands the postulation of an uniform medium of infinite extend as shown in left hand side of fig.5.8. This condition is rarely encountered in practice. The right hand side of the figure shows the possible distortion of the current pattern that occurs due to the presence of low resistivity layers. The electrode arrangement shown in figure 5.8 is used in the "normal" device. The distance AM is called the spacing. Two spacings are utilised: the "short" normal (AM = 16 inches) and the "long" normal (AM = 64 inches) for shallow and deeper investigation respectively. In actual practice all 4 electrodes are located in the hole. Electrodes B and N are placed at sufficiently great distances from the AM group to ensure a negligible effect on the potential measured between M and N. In the so-called LATERAL device, the M and N electrodes are placed close together compared with their distance from A to M. The spacings is very long (18 ft 8 in) as indicated in figure 5.9. This allows a deep investigation. Consequently the tool has a very poor vertical resolution and a marked asymmetric response. Note, B is the return electrode.

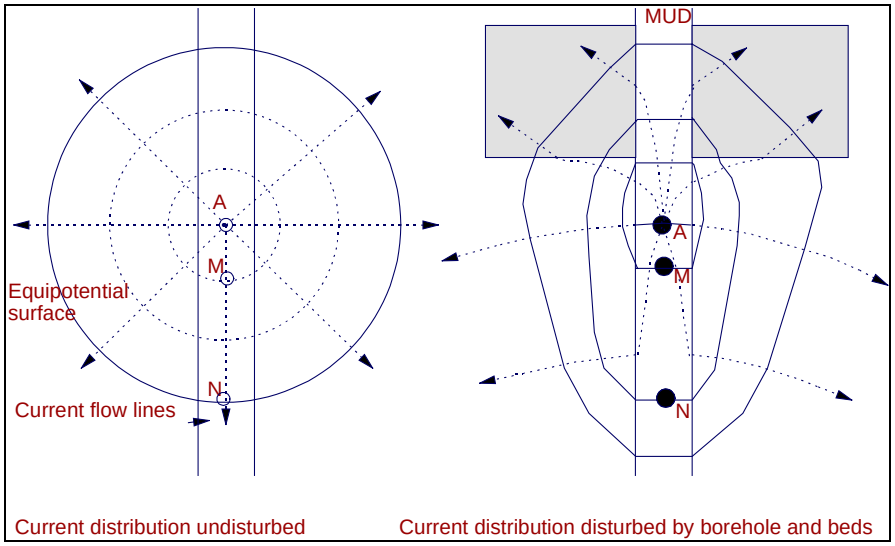

Figure 5. 8: Current distribution with and without a borehole/layer disturbance

5.3.2.2 SN, LN AND LATERAL LOG BEHAVIOUR

The short normal is widely used for geological correlation between wells and provides an fair value of R_{xo}. The long normal and lateral are adapted to supply a reasonable value of R_t in thick beds. Normally homogeneous resistive layers are alternating with low resistivity beds. The tool response in thick resistive beds shows:

- poor bed definition (rounding off) when the bed thickness is smaller than the tool spacings AM
- apparent bed thickness smaller than actual thickness by an amount equal to AM.
- a thin resistive layer is reflected by a depression together with two symmetrical peaks.

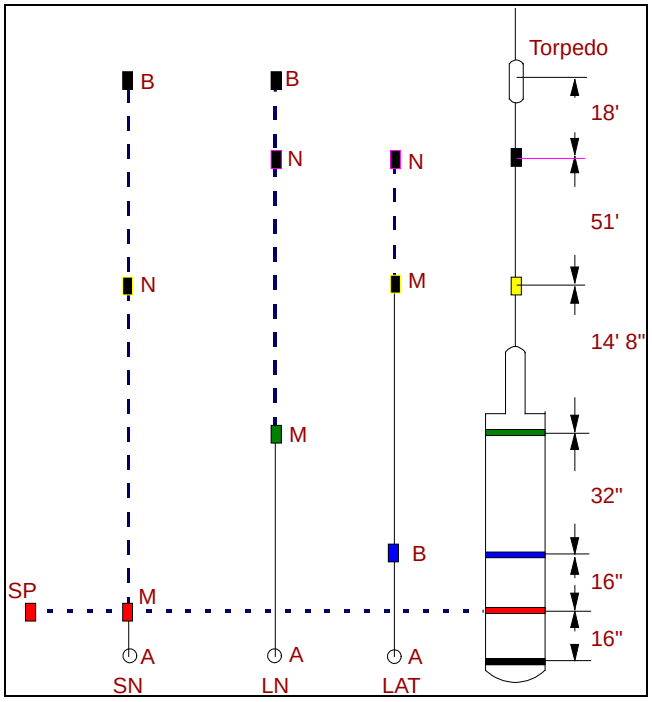

Figure 5.9: The electric sonde with SN, LN and Lateral.

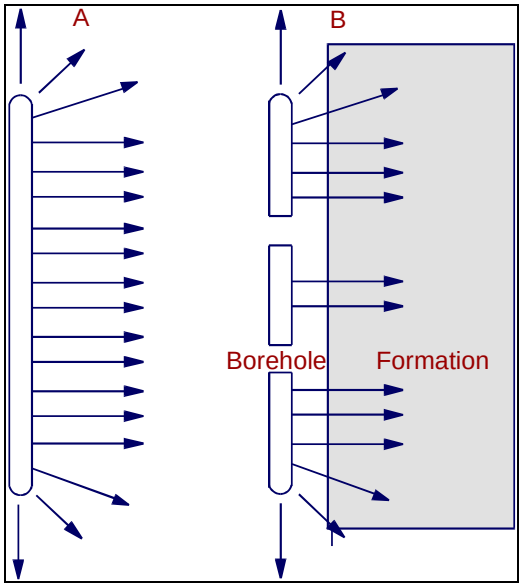

Figure 5.10: Pattern of current flow from a long cylindrical electrode located in a homogeneous medium

5.3.3 LATEROLOG TOOLS (LL3, LL7 & DUAL LATEROLOG)

Logging with laterologs was introduced to cope with salty mud. These muds have a very high conductivity, and consequently the effect of the borehole on resistivity measurements is also very high. The Laterolog technique is therefore complementary to the induction logging method, designed for oil-base mud which has hardly any conductivity at all.

5.3.3.1 LL3

Figure 5.10 shows the principle of the focused current log. On the left a long electrode bar is shown imbedded in a homogeneous medium. The potential is constant all over the bar and the current lines will run horizontal in the middle because current flow lines are perpendicular to equi- potential surfaces. The same principle is applied for the LL3 by using 3 bars as shown at the right in figure 5.10. The centre bar is 1 foot long and the two guard electrodes are 5 feet. By keeping the potentials equal for all three electrodes the current from the middle one is forced horizontally into the formation. This is even true when the bars are surrounded by a layer of mud with a resistivity that is much lower than the resistivity of the formation. The currents of the guards are adjusted to maintain the same potential as the centre electrode, while the potential of the centre electrode is kept at a fixed value. The ratio of the current and the potential of the centre electrode is a good indication of the formation conductivity C_t.

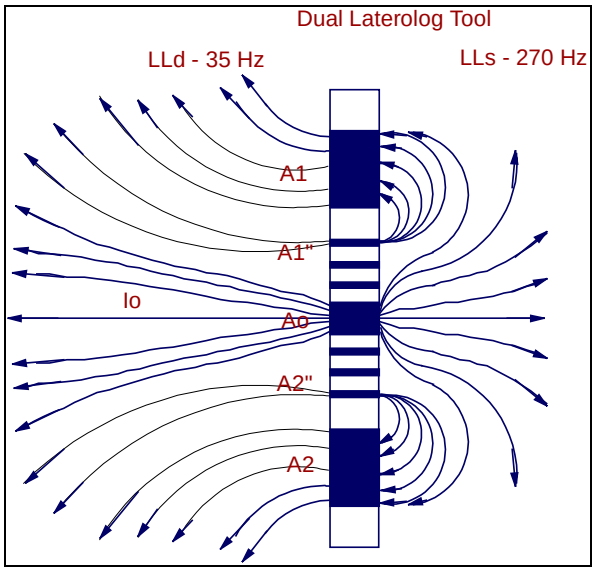

Figure 5. 11: The Dual Laterolog configuration

5.3.3.2 LATEROLOG 7 (LL7)

The laterolog 7 (LL7) is based on the same design as the LL3. In the LL3 the electrodes that carry very high currents (several amperes) are also used to measure potentials. This restricts the dynamic range of the measurements. In the LL7 two separate potential measuring electrode pairs are added, bringing the total to 7. The return electrode is positioned far away from the tool on the logging cable. This lay-out ensures that the current sheet penetrates the invaded zone and improves the measurement of the resistivity of the uninvaded zone.

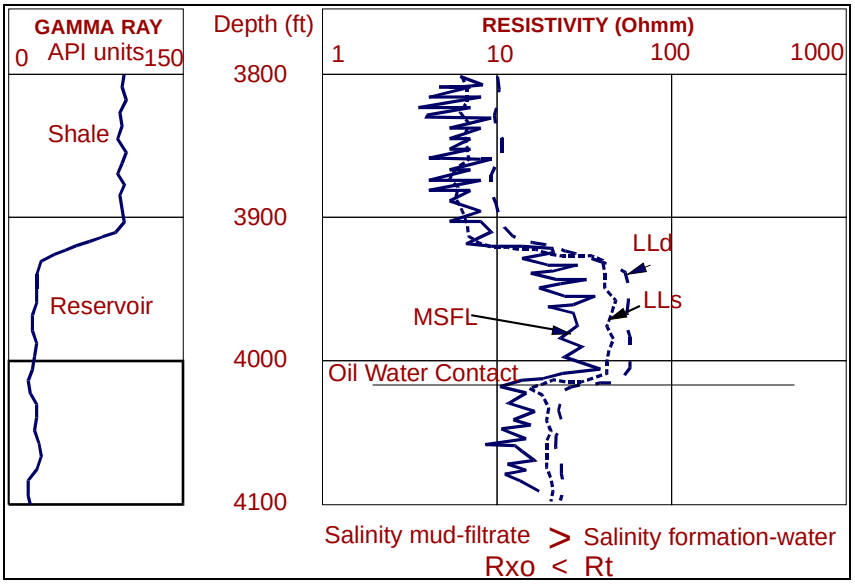

Figure 5. 12: Example of investigation depth of the Dual Laterolog

5.3.3.3 DUAL LATEROLOG

The dual laterolog is a combination of deep (LL_d) and shallow (LL_s) investigation devices. The principles adopted in the LL7 and LL3 have been combined in one tool, which features the 7 electrodes in its centre and 2 large bucket electrodes positioned respectively above and below the series of 7. In the LLd (deep) mode (left of figure 5.11), the surveying current I_o , that flows from the centre electrode, is focused by bucket currents from electrodes A1 and A2 supported by A1" and A2". The four "A" electrodes are all connected in this mode. This arrangement provides strong focusing deep into the formation. In the LL_s (shallow) mode (right-hand part of figure 5.11) the bucking currents flow from A1 to A1" and A2 to A2", reducing the depth of investigation. The electrodes are switched several times per second from one to the other configuration and the two resistivity traces are produced simultaneously. The dual laterolog measurements are often supplemented with a shallow resistivity measurement carried out with electrodes that are mounted in a pad which is pressed against the borehole wall to obtain R_{xo}. In this way three resistivity measurements are obtained simultaneously with different radii of investigation. An example is shown in figure 5.12. This situation is representative for invasion by mudfiltrate with a lower resistivity (higher salinity) than the original formation water. The LL_s is more affected by the invaded zone than the LL_d, while the MSFL reads very shallow in the order of 2-4" and gives a very good approximation of the low resistivity of the invaded zone.

5.3.4 INDUCTION LOGGING

The induction log, originally designed for resistivity recording in wells drilled with non-conductive fluids, has found its widest application in holes drilled with fresh and oil based muds. The sonde contains at least 3 coils, one transmitter and two receiver coils (figure 5.13). The transmitter sends out an alternating current with a frequency of 20 kHz of constant intensity. The alternating magnetic field generated by the primary coil induces secondary ground current loops in the formation. These loops in turn create magnetic fields, which induce currents in the receiver coils. The amplitude of the secondary field is proportional to the conductivity of the formation. The two receiver coils R1 and R2 are wound in opposite directions to compensate the direct coupling between T and R1. Actual

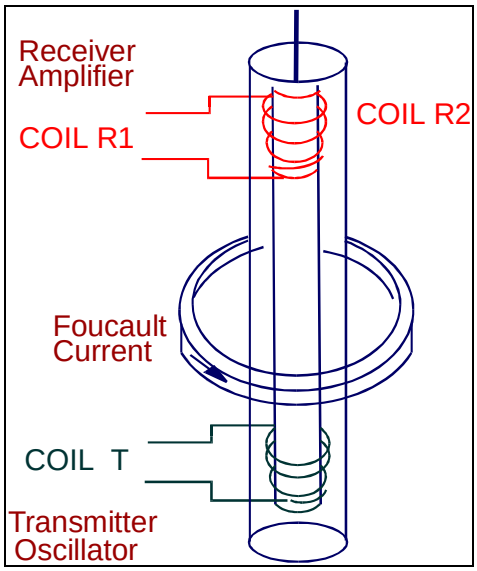

Figure 5. 13: Principle of the Induction Tool

logging tools contain 4 to 16 coils, of which the signals are combined to improve the vertical resolution as well as obtain a range of investigation depths (focusing).

An example of an induction log recording with deep (IL_d) and medium (IL_m) investigation depths is shown in figure 5.14, together with a shallow laterolog (LL_s) resistivity curve, and the spontaneous potential curve that will be discussed in the next chapter. The resistivity logs in figure 5.14 indicate the presence of a hydrocarbon/water contact, here denoted as oil/water contact. The shallow reading laterolog reading LL_s measures a higher resistivity than the induction log medium, which in turn measures higher than the deep induction log. This situation is representative for invasion by mudfiltrate with a higher resistivity (higher salinity) than the original formation water. The LL_s is more affected by the invaded zone than the IL_m, while the IL_d is usually hardly affected by the invaded zone.

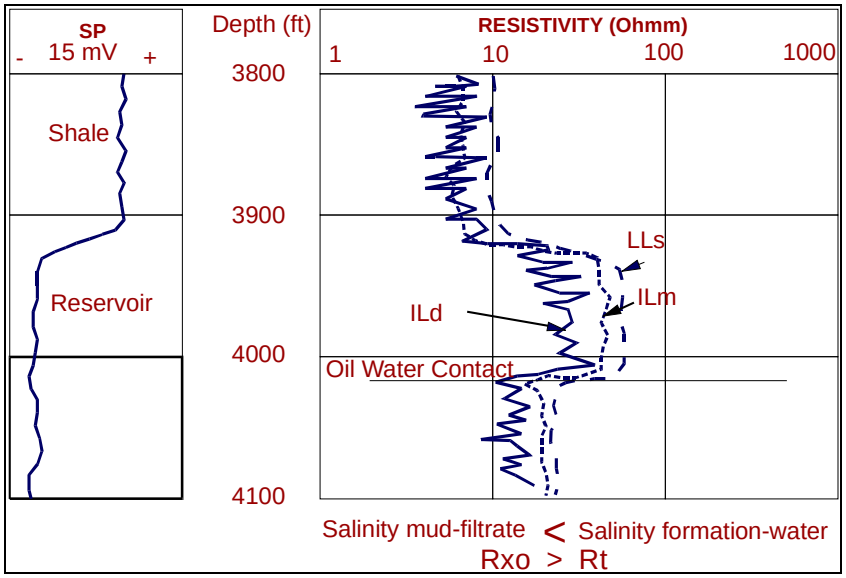

Figure 5. 14: A section recorded by the Dual Induction (DIL) Shallow Laterolog

5.3.5 MICRO-RESISTIVITY DEVICES

These tools are characterised by their short electrode distances of a few inches, which permit very shallow investigation. The micro-resistivity devices provide therefore usually a good approximation of the resistivity R_{xo} of the flushed zone. To avoid that the tools would only read the mud resistivity it is necessary to maintain physical contact between the electrodes and the formation. All tools in this category are therefore equipped with an electrode pad, which is pressed against the borehole wall, and designed to plough through the mud-cake.

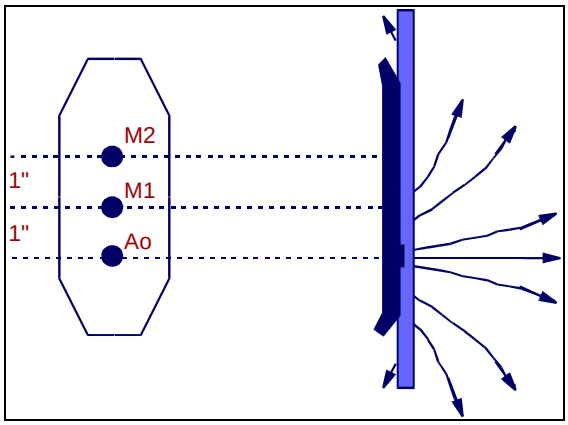

Figure 5. 15: The microlog principle

5.3.5.1 THE MICROLOG (ML)

This tool has 3 small button-shaped electrodes that are embedded in a rubber pad (figure 5.15). The electrodes are placed in a vertical line with a spacing of 1 inch between the successive electrodes. A current of known intensity is emitted from A_o and the potential differences between M_1 and M_2 and between M_2 and a surface electrode is measured. The resulting 2 curves represent a 2 inch

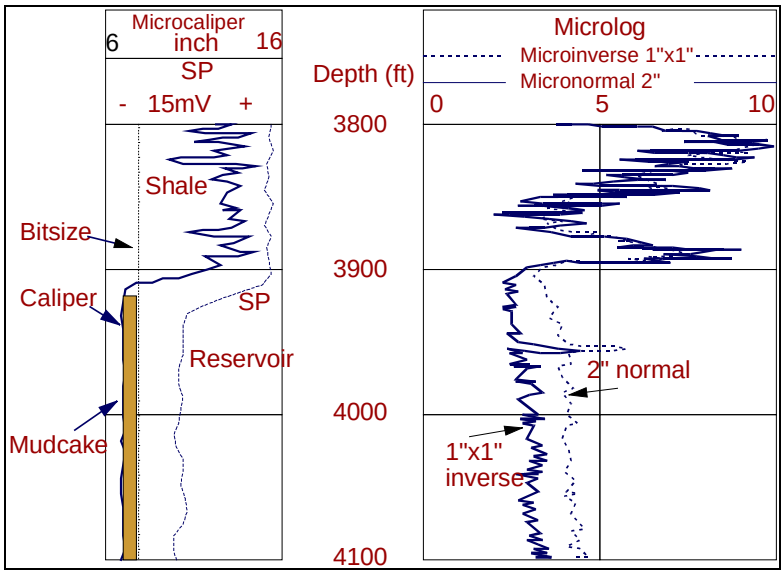

Figure 5.16: A MLC or Microlog Calliper example

normal and 1 inch "inverse" recording. The radius of investigation is smaller for the inverse, which is therefore strongly affected by the mudcake. The normal curve reads 2 to 3 inch deep and is therefore more affected by the invaded zone.

The mudcake usually has a lower resistivity than the permeable beds, and the "inverse" will therefore read a lower value than the normal. Consequently, the ML detects mudcake by showing a separation between the 2 resistivity traces and thereby delineates the permeable beds. The ML is the best of all micro devices for making "sand counts". In figure 5.16 a section of the ML is shown. The separation of the micro normal and micro-inverse clearly shows the permeable bed delineation. This is confirmed by the separation between the calliper and the nominal bit size, which gives the mudcake thickness.

5.3.5.2 MICRO SPHERICALLY FOCUSED LOG (MSFL)

This device is incorporated in the dual laterolog DLL-R_{xo} tool. Its design is based on the concept that accurate resistivity data can only be obtained when the potential distribution around the current emitting electrode is spherical. This condition has been approximated by an array of concentric electrodes that resembles the Dual Laterolog in cross section as represented in figure 5.17. Note that both contain 9 electrodes. Both, the investigating current I_o and the bucket current I_1 are in this case emitted through centre electrode A_o. The sum of these two currents is adjusted by varying the potential of electrodes A_1 and A_2 in such a way that the measured voltage at M_o is kept equal to a constant reference voltage. I_o is roughly proportional to the conductivity of the slice of the formation that is shaded in figure 5.17. The main advantage of the MSFL over the micro-log is that it is much less affected by the mudcake. Therefore it gives a better estimate of the flushed zone resistivity R_{xo}, which is derived with equation.5.21:

$$R_{xo} = \frac{E_{Mo} - E_{M1}}{I_O} \qquad \text{(eq. 5.21)}$$

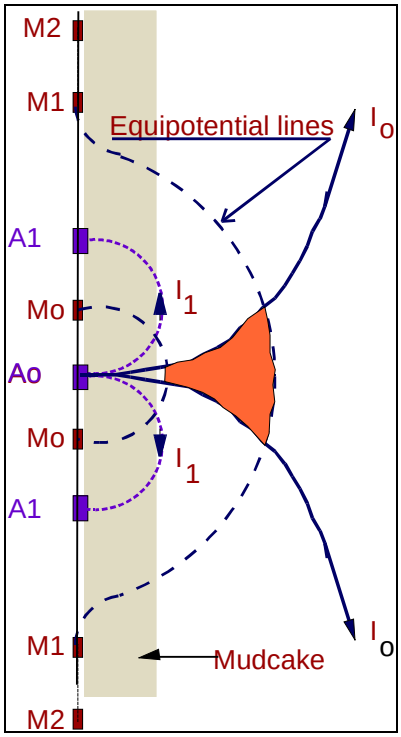

Figure 5. 17: Micro-SFL principle (After Schlumberger)

5.3.6 VERTICAL AND HORIZONTAL RESOLUTION: SUMMARY

In table 5.3 a summary of the depth of investigation of the resistivity tools is given. The values are rounded off in feet. These are only indicative values and it is emphasised that the actual investigation of the resistivity tools is a function of the resistivity of the mud, mudfiltrate, formation water, hydrocarbon content, porosity, borehole size and other parameters, like rock type, etc..

Depth of investigation resistivity tools	**Vertical**	**Horizontal**
(Figures are rounded off in feet)	**(ft)**	**(ft)**
SN (Short Normal)	1.5	1.5
LN (Long Normal)	5	5
Lateral	20	20
ILD Induction deep (6FF40)	6	10
ILD Induction (6FF27)	4	4
ILM Induction medium	5	6
LLD (Laterolog Deep)	2	10
LLS (Laterolog Shallow)	2	2
LL3 (Laterolog 3)	3	4
LL7 (Laterolog 7)	3	4
MLI (Microlog Inverse 1 x 1")	0.2	0.2
MLN (Microlog Normal 2")	0.3	0.3
MLL (Micro-Laterolog)	0.5	0.5
MSFL (Micro-SFL)	1	0.5

Table 5. 3: : Summary of the depth of investigation of the resistivity tools

5.4 NATURAL ELECTRICAL POTENTIAL

5.4.1 ELECTRICAL POTENTIAL AND OCCURRENCE

Electrical exploration involves the search of properties created by electric current flow in the rock, recognised at a surface. Using electrical methods, one can measure natural or artificial potentials, currents and electromagnetic fields in the rock. It is the large difference in electrical conductivity of various rock/mineral types that make the electrical methodologies feasible. Electrical methods that use a natural source are; self-potential, telluric currents/magnetotellurics, audio-frequency magnetic fields and resistivity.

Several electrical properties of rocks and minerals are significant in electrical prospecting. They are natural electrical potentials, electrical conductivity (or the inverse, electrical resistivity) and the dielectric constant. In this chapters we will study the electrical potentials of rocks and minerals. Certain natural or spontaneous potentials phenomena in the subsurface are induced by electrochemical or mechanical activity. Normally the controlling factor is the presence of fluid matter in the sub-surface (fig. 5.18). Potentials are associated with:

- weathering of (sulphide) mineral bodies,
- variation in rock properties (mineral content) at layer contacts,
- bio-electric activity of organic material,
- corrosion,
- thermal and pressure gradient

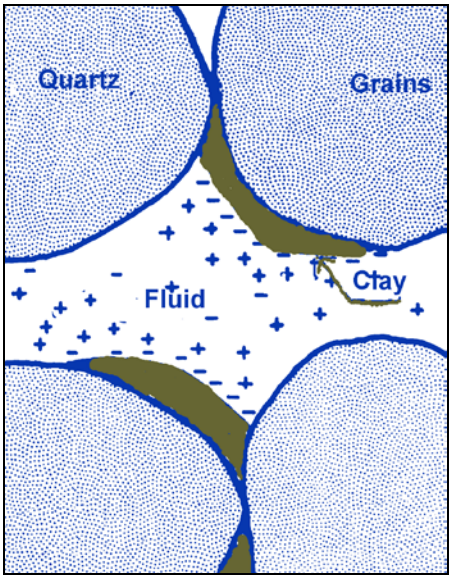

Figure 5.18:Example of charge distribution between minerals

5.4.2 ORIGIN OF ELECTRICAL POTENTIALS

One mechanical mechanism and three chemical mechanisms produce these potentials:

1. **Electrokinetic potential or streaming potential:** This is a well known effect that is shown when a solution of electrical resistivity and viscosity is forced through a capillary or porous medium.
2. **Liquid-junction (or diffusion) potential:** This is due to the difference in mobility of various ions in solutions of different concentrations.
3. **Shale (or Nernst) potential:** When two identical metal electrodes are immersed in a homogeneous solution, there is no potential difference between them. However, if the concentration at the two electrodes varies, then there is a potential difference. This associated diffusion and Nernst potentials are also known as the electrochemical, or static self-potential.
4. **Mineralization potential**. Two different metal electrodes dipped in an aqueous concentration give a potential difference. This electrolytic contact potential and the static self-potential cause large potentials associated with layers and mineral zones. They are known as mineralization potentials. These potentials, usually in zones containing sulphides, graphite and magnetite, are large when compared to the potentials of the preceding sections.
5. Further the magnitude of the static self-potential depends on **temperature**. This thermal effect is resembling to the pressure difference in streaming potential and is of minor importance.
6. **Erratic potentials,** sometimes present, are:
   - Metal corrosion (underground pipes, cables, etc.)
   - Large-scale earth currents induced from the ionosphere, nuclear blasts, thunderstorms
   - Currents of bio-electric origin flowing, for instance, in plant roots are also a source of earth potentials.

Most of the earth potentials discussed above are relatively permanent in time and place.

5.4.3 METHOD OF APPROACH AND APPLICATIONS

In a comprehensive way; for the interpretation of borehole information on groundwater, formation water and minerals, electric currents are propagated in rocks and minerals in three ways:

a) electronic: The first is the normal type of current flow in materials containing free electrons, such as the metals.

b) electrolytic: In an electrolyte the current is carried by ions at a comparatively slow rate.

c) dielectric: Dielectric conduction takes place in poor conductors or insulators, which have very few free carriers or none at all. Under the influence of an external varying electric field, the atomic electrons are displaced slightly with respect to their nuclei; this slight relative separation of negative.

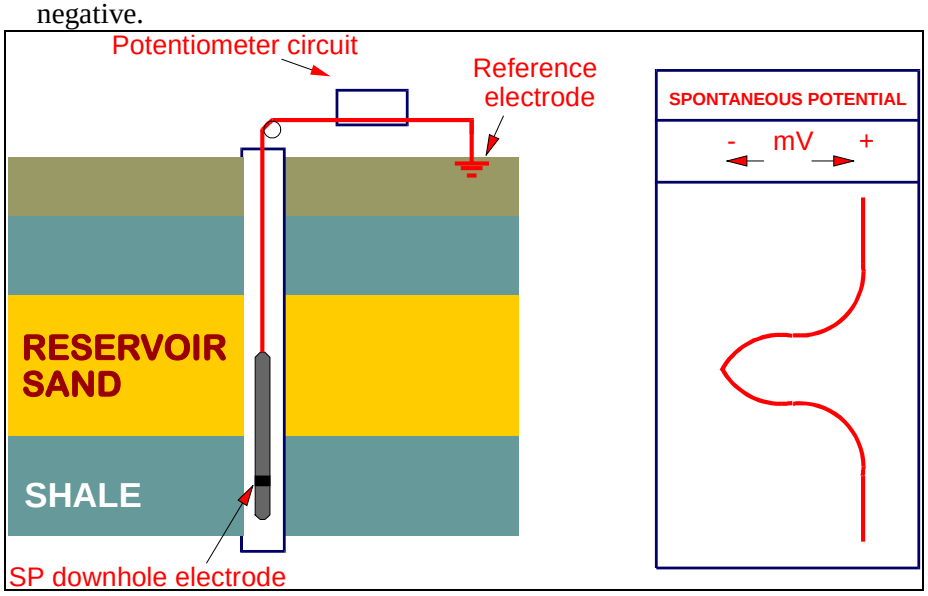

Figure 5.19: Sketch of a spontaneous potential measurement in a drill hole

The spontaneous potential (or SP) curve reflects the potential difference between a movable electrode in the borehole and a fixed reference electrode at the surface as depicted in figure 5.19. In the shale zone the SP readings are usually fairly constant and tend to follow a straight line, called the **shale base line**. In the sandy zone or in permeable formations the SP shows deviations from the shale base line to one or more **sand line** levels. Depending on the relative salinity of the formation water and the mudfiltrate, the deflection may be to the left or the right of the shale base line. The SP effect is produced by two components : the electro-chemical and the electro-kinetic potentials.

The main applications for SP-measurements are:

- Groundwater control
- Determination of formation water resistivity
- Determination of the environment of deposition
  - Evaluation of lithologies such as shale and coal
  - Determination of the shale content of a layer
- Detection of permeable beds and their boundaries
- Well to well correlation

5.5 THE ELECTROCHEMICAL COMPONENT

The electro-chemical component *Ec* consists of the Liquid junction potential (*Ej*) and the membrane potential (*Em*). These potentials create a current that flows at the shale - reservoir interface. When a reference electrode is moved across this interface a potential difference is measured.

The mud-weight is usually higher than the formation fluid pressure. This produces an over-pressure at the face of the reservoir exposed by the borehole and causes mudfiltrate to invade the reservoir.

Thereafter a mudcake is formed and the fluid invasion slows down. An invasion profile as shown in Figure 5.20.b. is formed. In this case the mudcake separates a high saline formation water and a low salinity mudfiltrate.

5.5.1 LIQUID JUNCTION POTENTIAL

The liquid junction potential Ej is created at the interface between the invaded and the uncontaminated zone, due to a salinity difference between mud filtrate and formation water. Since the negative Cl^- ions, assuming a NaCl solution, have a greater mobility than the positive Na^+-ions, the net result is a flow of negative charges, of Cl^- ions, from the more concentrated solution to the less concentrated solution. This mechanism, driven by the conductivity difference the mudfiltrate and formation water, is further explained in figure 5.20.c.

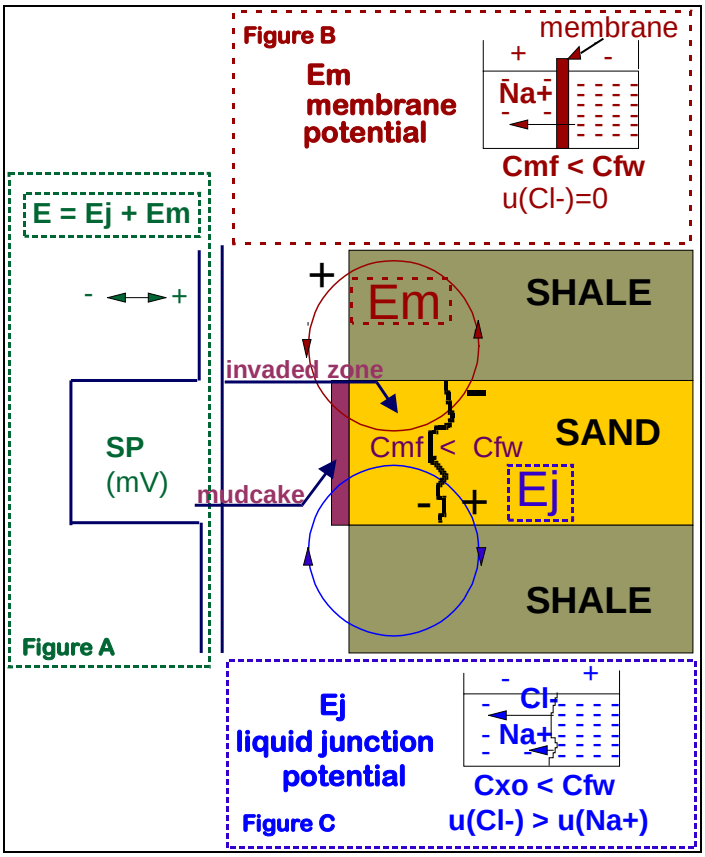

Figure 5. 20: Scheme of potentials measured with the SP.

5.5.2 MEMBRANE POTENTIAL

Figure 5.20.b shows that the membrane potential "Em" is functioning across the shale, between the uncontaminated zone in the reservoir and the mud in the borehole. Shales can act as membranes, which means that they are permeable for one type of ion and a barrier for other types. This property is called ionic perm-selectivity. Its result is that the shale-membrane can preferentially prevent the movement of negative ions. Shales are cation exchangers; they are electro-negative and therefore repel anions. In most instances the shales are 100% effective and therefore repel all the chlorine ions. The positive sodium ions move toward the lower salinity mud in the borehole and the chlorine ions cannot follow this movement. As a result a positive potential is generated toward the low concentration NaCl solution.

Considering that at the interface shale / reservoir a current is created by the Ej and Em potentials which act in series. Ej has a positive value toward the uncontaminated zone containing formation water. In contrast Em is positive toward the mud in the borehole, which has the lower NaCl concentration.

The magnitude of both the liquid junction potential and the membrane potential depends on the difference in ion concentration of the mud (filtrate) and the uncontaminated formation water. Both they can be expressed as :

$$E = k.log\frac{Con_w}{Con_{mf}} \qquad \text{(eq. 5.22)}$$

Here Con_W and Con_{MF} are the ion concentrations in respectively the formation water and the mudfiltrate that produce the Ej and Em potentials. Con_W and Con_{MF} are inversely proportional to respectively the resistivity *Rw* of the formation water and *Rmf* the resistivity of the mudfiltrate. The

constant *k* is different for the *Ej* and the *Em* potential but the equivalence of the relations allows the combination into one effective potential E:

$$E = E_j + E_m = (-71).log\frac{R_{mf}}{R_{wf}} \qquad \text{(eq.5.23)}$$

With *E* expressed in mV, and the factor (-71) as the combination of the "*k*" constants. Normally the resistivity of the mudfiltrate *Rmf* is measured at the wellsite at room temperature. The SP measures the potential *E* at borehole temperature and the *Rmf* should therefore be corrected for this temperature difference. Using equation 6.2 and the measured values for *E* and *Rmf*, the resistivity of the uncontaminated water in the formation *Rw* can be calculated. From the value of *Rw* the formation water salinity can be derived taking into account the reservoir temperature.

5.6 ELECTROKINETIC COMPONENT

In the foregoing the "streaming potential" caused by the movement of the mudfiltrate through the mudcake has been ignored. Like the shale layers, the mudcake acts also as a membrane that hinders the movement of the negative ions. A potential difference "*Ek*" is thereby generated, and the SP has to be corrected for this electrokinetic component. The value of *Ek* can be obtained from laboratory experiments with various muds that are in common use. For modern muds that seal the formation very effectively the streaming potential *Ek* can often be ignored.

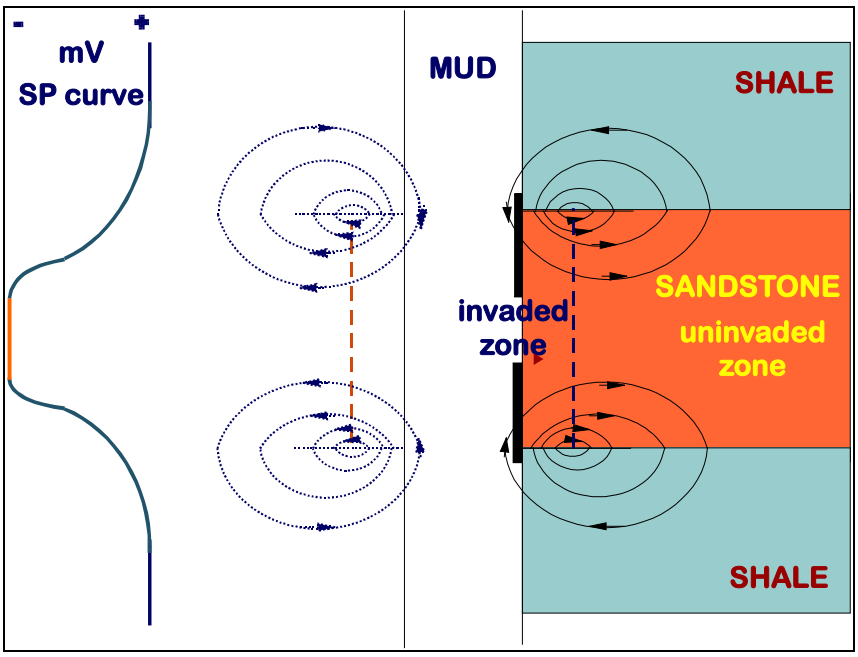

Figure 5. 21: Currents created in the mud, invaded zone, shale and sandstone, by the *Ej* , *Em*, and *Ek*.

5.7 THE COMBINATION OF SP COMPONENTS

The combined junction- , kinetic-, streaming- and membrane potentials, create a current through the shale/reservoir interface, as illustrated in figure 5.21. The currents created by this series of potentials flow through 5 different media, each with its own resistivity:

1. the borehole filled with mud (*Rm*),
2. the mudcake (*Rmc*),
3. the invaded zone filled with mudfiltrate (*Rxo*),
4. virgin zone filled with uncontaminated fluids (*Rt*),
5. the surrounding shales (*Rsh*).

In each medium the potential along a line of current flow (*I*) drops in proportion to the resistance that is encountered.

$$E_{total} = I \cdot R_m + I \cdot R_{mc} + I \cdot R_{xo} + I \cdot R_t + I \cdot R_{sh} \qquad \text{(eq.5.24)}$$

Hence, the driving force behind the potential (E_{total}) can be expressed as :

$$E_{total} = E_m + E_j + E_{kmc} + E_{ksh} \qquad \text{(eq. 5.25)}$$

As mentioned in the previous section the streaming potentials E_{kmc} over the mudcake and E_{ksh} through the shale are often ignored. The SP often is used to estimate the groundwater or formation water salinity in exploration wells in which no production has taken place, and formation water

Clay	Density (g/cm^3)	Hydrogen (%)	Average Q_{CEC} (meq/g)
Kaolinite $Al_4(Si_4O_{10})(OH)_8$	2.69	1.5	0.03
Illite $K_{1-1.5}Al_4(Si_{6.5-7.0}\ Al_{1-1.5}O_{20})(OH)_4$	2.76	0.5	0.20
Montmorillonite $(½Ca,Na)_{0.7}(Al,Mg,Fe)_4(Si,Al_8O_{20})(OH)_4$	2.33	0.5	1.0
Chlorite $(Mg,Al,Fe)_{12}(Si,Al)_8O_{20}(OH)_{16}$	2.77	1.2	0.0

Table 5. 4: Clay properties that contribute to changes in the spontaneous potential of shaly sediments.

samples have not been analysed.

5.8 SHALE VOLUME CALCULATION

The presence of shale in the reservoir suppresses the SP. The shale volume can be calculated from the SP as follows :

$$V_{sh} = \frac{PSP - SSP}{SSP} \qquad \text{(eq. 6.5)}$$

with,

Vsh : the shale volume as fraction of the bulk volume in %

PSP : the SP log reading of a shaly reservoir as a deflection from the shale base line corrected for environmental effects such as mud resistivity Rm,. The SP electrode only measures a potential deflection while travelling uphole (*SP=I x Rm*).

SSP : the SP log reading in a clean reservoir as the deflection from the shale base line corrected for environmental effects. The SSP can be obtained by taking the SP reading in the thickest and cleanest reservoir.

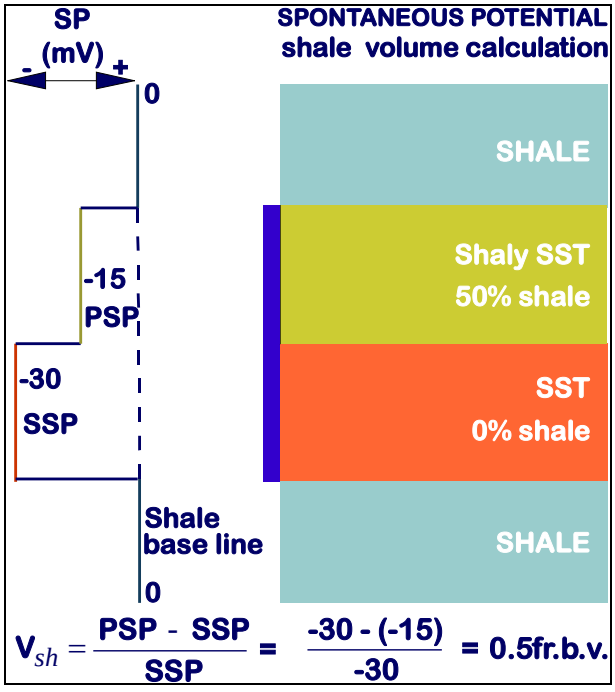

Figure 5.22: Shale volume calculation example using the SP

5.9 GEOLOGICAL INFORMATION

The environment of deposition is often indicated by the log shape. Examples for a channel sand, barrier bar, beach sand and deltaic section are shown in the figures 6.6 a-d. As shown, the grain size plays an important role. At low energy sedimentary environments a higher amount of clays can be deposited. As shown, the contribution of clays in the sub-surface and related formation water content, also gives an extra contribution to the E_{ksh}.

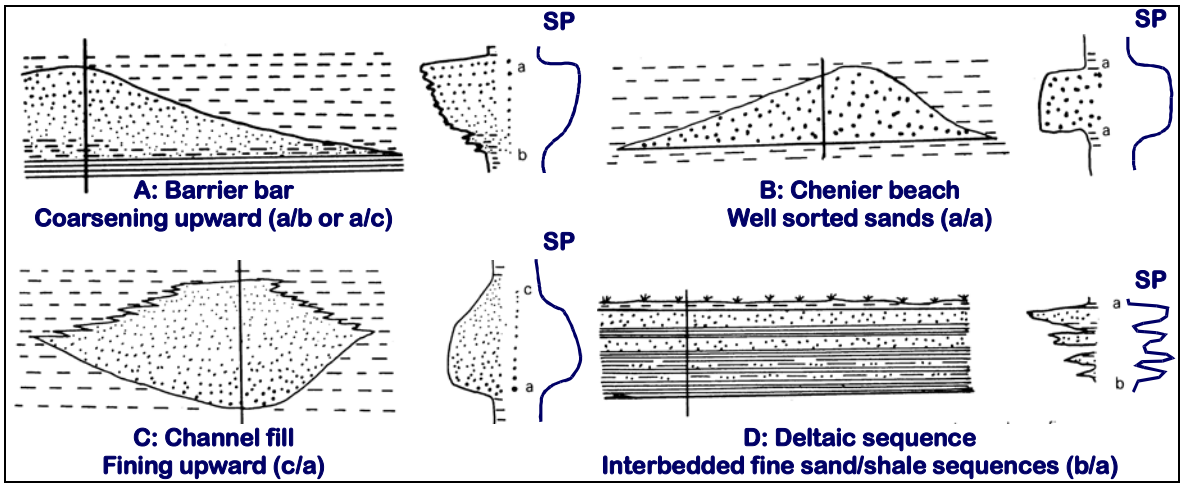

Figure 5. 23: Typical geometries of SP-curves for sandstone environments (revised after Tizzard et al., Bull. Can. Petr. Geol., 1975)

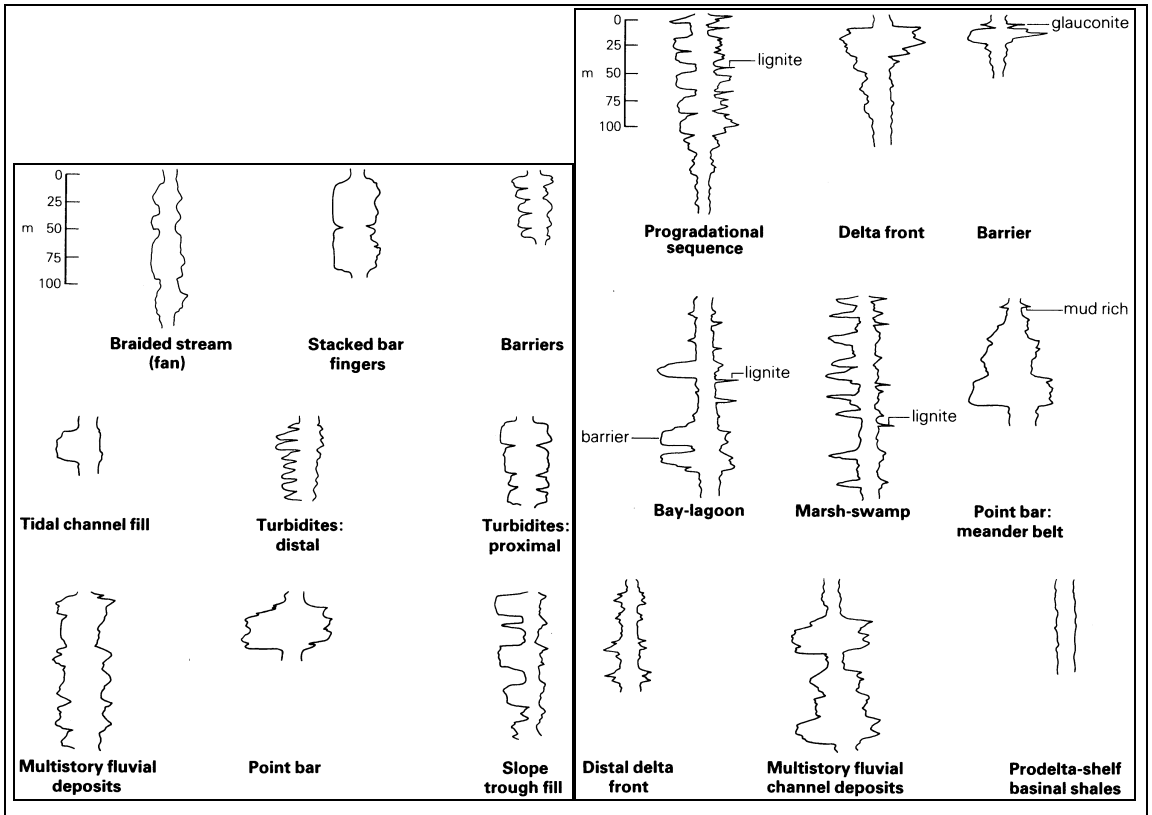

Figure 5. 24:Schematic representations of SP/Resistivity log patterns: The left group shows sand rich depositions; note the blocky appearance. The right group shows the variety of sand/shale depositional environments. (revised after Gracia, AAPG bull., 1981)

As shown in figure 5.23, shale content determines the shape of the SP-curve. For this reason many sedimentary environments are characterised on their SP-shape. During a log-analysis and correlation session, all wells in a certain geological area, can be correlated, in order to define the lateral continuity of shales, sands and other rock types. The figures 5.24 and 5.25 show various type curves for both, SP and resistivity logs.

5.10 THE EFFECT OF THE SHALINESS - Q_V

As shown, the SP is very sensitive to the presence of shale or clay in permeable formations, in which only the electrochemical contribution is affected. As already shown in figure 5.18 and 5.25, clay or phyllosilicates, do have highly reactive surface exchanging ions, such as Ca, Mg, K, Na, etc., which create an additional conductivity. This conductivity is expressed as the "Cation Exchange Capacity", or CEC, which can be defined as:
The amount of positive ion substitution that occurs per unit weight of dry rock. This expression is valued in units milli-equivalents per one hundred grams of dry rock; meg./100 g. In equations CEC is expressed as "Q_V", which is defined as the cation-exchange capacity per unit pore volume; meq/l.

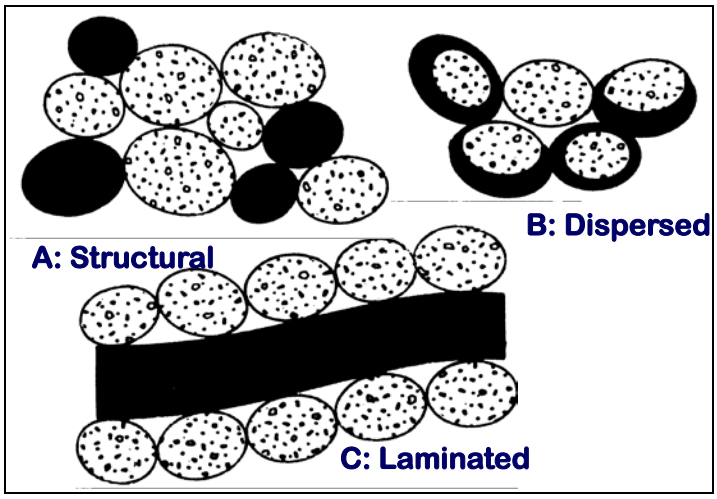

Figure 5. 25: Three types of clay distribution in a permeous sand aggregate.

The Q_V of a pure shale is considered to be equal to 1. In the Shell laboratories, Q_V, the "Cation Exchange Capacity" was determined for a series of shales in relation to their water salinity (C_{NaCl}). The example in figure 5.27, shows such a relation

Three methods are valid for measuring the Cation Exchange Capacity:

1. **Conductivity measurements** at multiple fluid salinities. The method is non-destructive and described in the next section, that discuss the Waxman-Smits equation.
2. **The wet chemistry technique**: The method is destructive because the sample is grinded. Via a titration technique with ammonium acetate the number of positive exchange ions are established. The CEC increases for the same sample when the grinded particles become smaller. Therefore one has to be careful with this method.
3. **The membrane Potential**: The method is non-destructive by measuring the membrane-potential on a sample. Than the Q_V can be calculated.

The most reliable method is considered to be the conductivity method. Another method of obtaining the Q_V of a reservoir is solving the water-bearing equation in a water-bearing zone when the other parameters are known by other means.

5.11 A WATER SATURATION EQUATION: PRACTICE

The effect of clay is that it reduces the resistivity and consequently the derived hydrocarbon saturation calculated with Archie is too low. There are two types of saturation equations that can correct for the extra conductivity caused by the shale. The shale volume and cation exchange capacity method. Here we discuss the latter.

5.11.1 CEC BY WAXMAN-SMITS

The first CEC-method was developed by Waxman and Smits (1968). Their equation relates the electrical conductivity of a shaly sand to the water conductivity and the cation exchange capacity per unit pore volume of the rock, Q_V. The method is assumed to be independent of the clay distribution.

5.11.2 WATER BEARING RESERVOIRS

The conductivity of the shaly water bearing sand is expressed by the equation:

$$C_0 = \frac{1}{F^*}\left(C_w + C_e\right) \qquad \text{(eq. 5.27)}$$

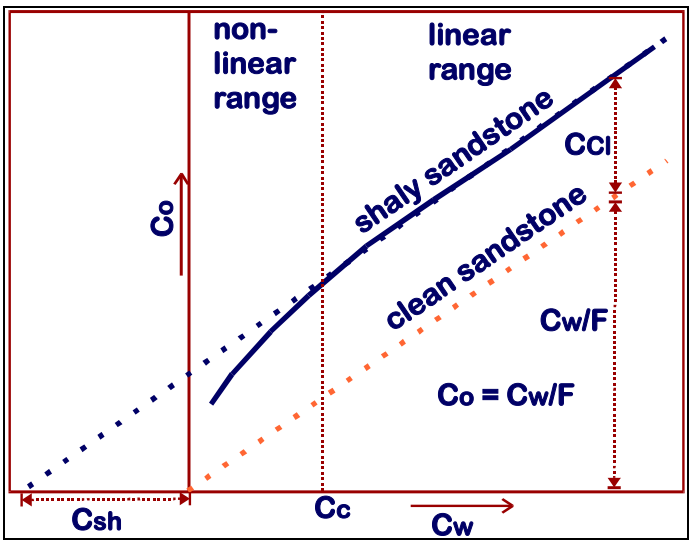

Figure 5.26: Relation between clean sand, clay content, formation conductivity and water conductivity.

where:

*F** : formation factor corrected for shale
Co : conductivity of 100% water-bearing reservoir, mmho/m
Cw : conductivity of the formation water, mmho/m
Ce : conductivity of the clay fraction, mmho/m

If *Co* and *Cw* are measured in the laboratory, then *F** and *Ce* can be obtained (figure 5.26) through:

$$Ce = B \times Qv \qquad \text{(eq. 5.28)}$$

with B as the equivalent conductance of the counter-ions as a function of the solution conductivity "*Cw*" in Ohm^{-1} cm^3 meq^{-1}. The *Ce* is obtained from conductivity measurements. It is plotted versus *Qv*, which is obtained from titration techniques, for a large number of samples. The slope is more or less linear. The original article suggests that the distribution of the clays is a mixture of each type that is available. Therefore B is assumed to be independent of type, distribution and/or amount of clay in the sample. In some areas locally valid relationships between *Qv* and the total porosity have been found from laboratory data. This allows the assessment of the *Qv* distribution throughout the reservoir column based on porosity log data. The usual values of *Qv* in shaly sands range from 0.01 to 2 meq cm^{-3}.

Empirical relationships between *B* and *Rw* have been established at various temperatures. It was found that at temperatures in between 50 and 200 °C (or 120-390 °F), the product of *Rw.B* is not dependent on temperature. Therefore it can be represented as a function of water salinity alone. For temperatures ranging from 120-390 °F, the empirical relation is:

$$B \times R_w = 13.5 \times Sal^{-0.70} \qquad \text{(eq. 5.29)}$$

With; S_{al} as the salinity in g/l NaCl equiv., and; *Rw* as the formation resistivity in Ohm.m. For temperature of about 80 °F (or surface conditions), the empirical relation changes to:

$$B \times R_w = 6 \times Sal^{-0.64} \qquad \text{(eq. 5.30)}$$

5.11.3 HYDROCARBON BEARING RESERVOIRS

In hydro-carbon bearing formations the exchange ions associated with the clay become more concentrated in the remaining pore water. This concentration, *Qv'*, is related to *Qv* and *Sw*, according to the equation:

$$Q_V^{'} = \frac{Q_V}{Sw} \qquad \text{(eq. 5.31)}$$

Using the equations 6.6 to 6.10 and combining them with the Archie equation gives:

$$C_t = \phi_t^{+m*} \times S_{wt}^{+n*} \times C_w \left(1 + \frac{Rw \times B \times Qv}{Swt}\right) \qquad \text{(eq. 5.32)}$$

where:

Ct : log reading of conductivity (mmho/m) corrected for borehole, bed thickness and invasion.
ϕ_t : total porosity, fraction of bulk volume
*m** : cementation factor corrected for shale effect
Sw :water saturation, fraction of pore volume
*n** : saturation exponent corrected for shale effect
Cw : formation water conductivity
Rw : formation water resistivity
Qv : cation-exchange capacity per unit pore volume, meq/ml.
Csh : shale conductivity, mmho/m

This equation is not a simple linear function and has to be solved by iteration. If *n** has not been established from core measurements, a value of 1.8 may be used for shallow and 2.0 for deeper sands (say below 6000 ft). Juhasz developed in 1981 the normalised Qv method as showed in equation 6.12:

$$C_t = \phi_t^{+m*} \times S_{wt}^{+n*} \times C_w \left(1 + \frac{Qvn}{Swt}\left[\frac{Ccw}{Cw} - 1\right]\right)$$

(eq. 5.33),

where: *Qvn* = *Qv*/*Qvsh*

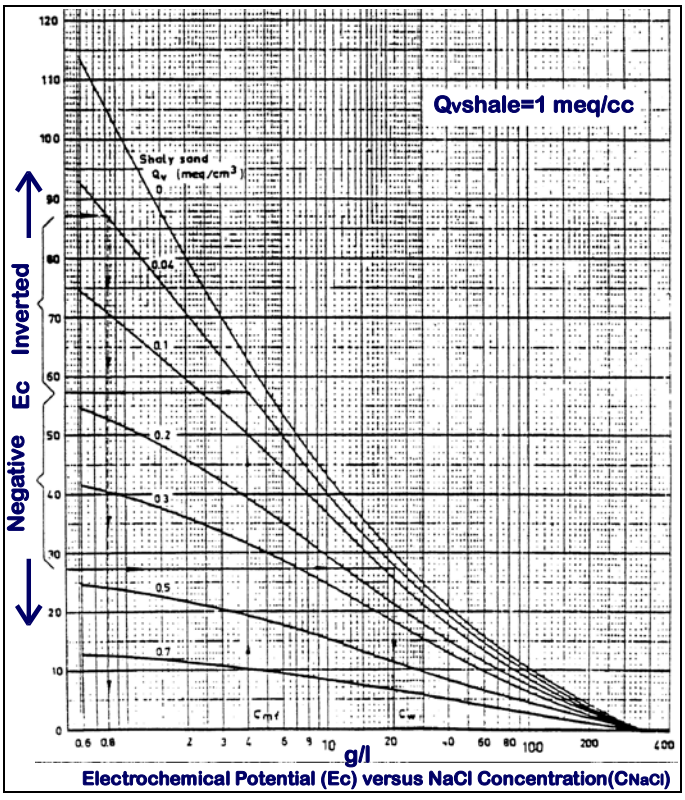

Figure 5. 27: Example of the effects of fluid salinity on the electrochemical potential.